Article

A HIGHLY SENSITIVE MOISTURE-RESISTANT BTEX SENSOR BASED ON POLYANILINE NANOFIBERS

Luyu Wang[a,*], Jia Song[b] and Chunyang Yu[c]
[a]College of Artificial Intelligence and E-Commerce, Zhejiang Gongshang University Hangzhou College of Commerce, 311599 Hangzhou, China
[b]School of Nuclear Science and Engineering, Shanghai Jiao Tong University, 200240 Shanghai, China
[c]Design-AI Laboratory, China Academy of Art, 310009 Hangzhou, China

Received: 02/23/2024; accepted: 06/10/2024; published online: 07/17/2024

The real-time sensing of benzene, toluene, ethylbenzene, and xylene (BTEX) vapor has become urgent due to their widespread hazards. As a sensing platform that combines low energy consumption and high sensitivity, moisture-resistant detection of ppb-level BTEX vapor remains a challenge for quartz crystal microbalance (QCM) based gas sensors. In this work, we employed polyaniline nanofibers as the sensing material, significantly enhancing the QCM sensor's detection capability for BTEX vapor down to the 50 ppb level. Besides, thanks to the hydrophobicity of polyaniline nanofibers, this sensor shows minimal response fluctuations to BTEX vapor in the relative humidity range of 50-90%. Furthermore, this sensor exhibits a short response time and excellent long-term stability, thereby presenting a broad prospect for future industrial applications in BTEX vapor detection.

Keywords: gas sensor; quartz crystal microbalance; BTEX; polyaniline nanofibers.

INTRODUCTION

The acronym BTEX stands for volatile organic compounds, including benzene, toluene, ethylbenzene, and xylene.[1-3] Widely employed in sectors like chemicals, petroleum, and coatings, they are recognized for their significant toxic and carcinogenic properties.[4-7] BTEX poses risks to the human respiratory, central nervous, and liver systems, and may lead to health complications like headaches, dizziness, and nausea.[8-10] Furthermore, BTEX plays a role in environmental contamination, heightening the likelihood of ozone layer thinning and worldwide climatic shifts.[4,11-13] Therefore, it is vital to rigorously oversee and manage BTEX emissions.

Gas sensors serve the purpose of identifying and quantifying air gas concentrations.[14-17] Typical varieties encompass sensors for electrochemistry, semiconductors, quartz crystal microbalance (QCM), among others.[18-20] Gas sensors by QCM provide acute sensitivity, swift reaction, and minimal energy use, facilitating accurate and instantaneous measurement of air gas concentrations.[21-23] By applying sensing materials to the QCM's electrode surface, it is possible to identify the target gas through their adsorption interactions.[24] Utilizing the QCM sensing platform, the primary sensing materials for detecting BTEX vapor are organic compounds, including polyvinyl acetate, polymer-plasticizer, polybenzimidazole, metal phthalocyanine, pentacene, poly(β-cyclodextrin-*co*-maleic anhydride), and organosilicate.[25-31] However, their ability to detect primarily lies in the ppm concentration, and the influence of environmental humidity is not mentioned. Therefore, it is necessary to design a novel QCM based BTEX sensing material that can detect ppb level concentrations in complex humidity environments, as it can optimize the performance parameters of such sensors and improve their practicality.

Polyaniline is a conductive and chemically stable polymer, with various synthesis methods including chemical oxidation and electrochemical synthesis.[32,33] Polyaniline nanofibers, with nano-sized dimensions, exhibit high surface area and tunable morphology.[34] Its unique conductivity, mechanical properties, and chemical stability make it highly attractive in catalysis, energy storage, sensors, and biomedical applications.[35-38]

Herein, we utilized polyaniline nanofibers as the sensing material, leading to a substantial improvement in the detection capability of the QCM sensor for BTEX vapor, achieving a sensitivity as low as 50 ppb. Due to the hydrophobic nature of polyaniline, this sensor demonstrates minimal variations in response to BTEX vapor within 50-90% relative humidity (RH). Additionally, this sensor exhibits a rapid response time and exceptional long-term stability, showcasing its significant potential in BTEX vapor detection.

EXPERIMENTAL

Chemical raw materials and devices

Details on the chemical substances employed in the synthesis of polyaniline nanofibers can be found in the Supplementary Material. Chengdu Westarace Electronic Co., China, supplied the QCM chip, adorned with silver electrode coating. Each QCM resonator is set to a standard frequency of 10^7 Hz (AT-cut).

Synthesis of polyaniline nanofibers

An in-depth explanation of the polyaniline nanofiber synthesis process is provided in the Supplementary Material.

Characterization, fabrication and test methods of the QCM sensor

Details on the instruments and methods employed for the characterization of polyaniline nanofibers; detailed descriptions of the production and examination techniques for the polyaniline nanofibers based QCM sensor; and the sensing evaluation system's scheme (Figure S1) are all available in the Supplementary Material.

*e-mail: Dr.Luyu-Wang@hotmail.com
Associate Editor handled this article: Lucia Mascaro

RESULTS AND DISCUSSION

Materials characterization

Scanning electron microscope (SEM) imaging was used to characterize the structure and dimensions of the polyaniline nanofibers created on the QCM substrate. As depicted in Figure 1a, the standard SEM depiction of the polyaniline nanofibers shows their consistent nanofibers, measuring around 100 nm in diameter. Figure 1b presents the outcome of the contact angle examination. When the contact angle between a water droplet and the surface of an object is greater than 90°, it indicates that the surface of the object is hydrophobic.[39] The contact angle of QCM substrates coated with polyaniline nanofibers is 111.61°, indicating its hydrophobicity.

Figure 2a displayed the X-ray diffraction (XRD) configuration of polyaniline nanofibers. Notice that the polyaniline nanofibers exhibited pronounced 2θ peaks at 20.62 and 25.43°, aligning with the reflective planes of (0 2 0) and (2 0 0) periodicity, which are parallel and perpendicular to the polymer chains, respectively.[40] Figure 2b illustrates the Fourier transform infrared (FTIR) spectra for polyaniline nanofibers. The oscillation patterns seen at 1582 and 1498 cm^{-1} are attributed to the elongation of aromatic C=C bonds found in quinone or benzene formations. The spectral band near 1302 cm^{-1} aligns with the C–N bond elongation vibration in aromatic secondary amines, while the 1145 cm^{-1} band is attributed to the N=Q=N vibration (with Q representing the quinone ring) exhibiting electron-like properties. The C–H bond in 1,4-disubstituted benzene exhibits an out-of-plane deformation vibration on the polyaniline linear main chain, observable at 826 cm^{-1}. The varied absorption bands observed between 3500 and 2800 cm^{-1} are mainly indicative of the elongation vibration in N–H bonds, stemming from secondary amine groups in polyaniline's backbone structure.[41]

Gas sensing properties

Tests were conducted on the polyaniline nanofibers based QCM sensor to assess its ability to detect BTEX concentrations between 50 and 800 ppb, as depicted in Table 1. The frequency shift values of the polyaniline nanofibers based QCM sensor to 50, 100, 200, 400, and 800 ppb of benzene vapor were –12.3, –23.7, –44.8, –82.3, and –160.5 Hz, respectively. The frequency shift values to 50, 100, 200, 400, and 800 ppb of toluene vapor were –20.1, –30.2, –48.5, –88.9, and –170.3 Hz, respectively. The frequency shift values to 50, 100, 200, 400, and 800 ppb of ethylbenzene vapor were –26.3, –42.7, –60.7, –93.3, and –178.8 Hz, respectively. The frequency shift values to 50, 100, 200, 400, and 800 ppb of xylene vapor were –27.7, –44.5, –63.6, –97.7, and –185.6 Hz, respectively. The aforementioned experimental findings suggest that the QCM sensor, made of polyaniline nanofibers, can identify concentrations of BTEX vapor at the ppb level.

Table 1. Frequency shift of polyaniline nanofibers based QCM sensor to BTEX vapor with various concentrations

Gas	Frequency shift / Hz				
	50 ppb	100 ppb	200 ppb	400 ppb	800 ppb
Benzene	–12.3	–23.7	–44.7	–82.3	–160.5
Toluene	–20.1	–30.2	–48.5	–88.9	–170.3
Ethylbenzene	–26.3	–42.7	–60.7	–93.3	–178.8
Xylene	–27.7	–44.5	–63.6	–97.7	–185.6

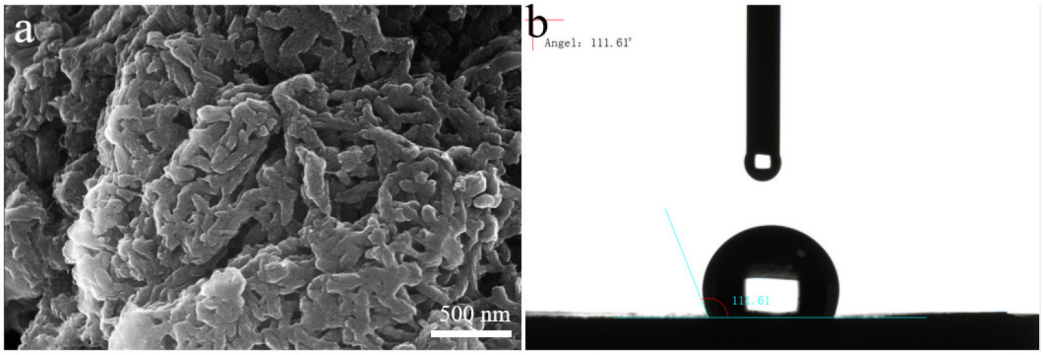

Figure 1. *(a) SEM image of polyaniline nanofibers coated on the QCM substrate; (b) contact angle test result of QCM substrates coated with polyaniline nanofibers*

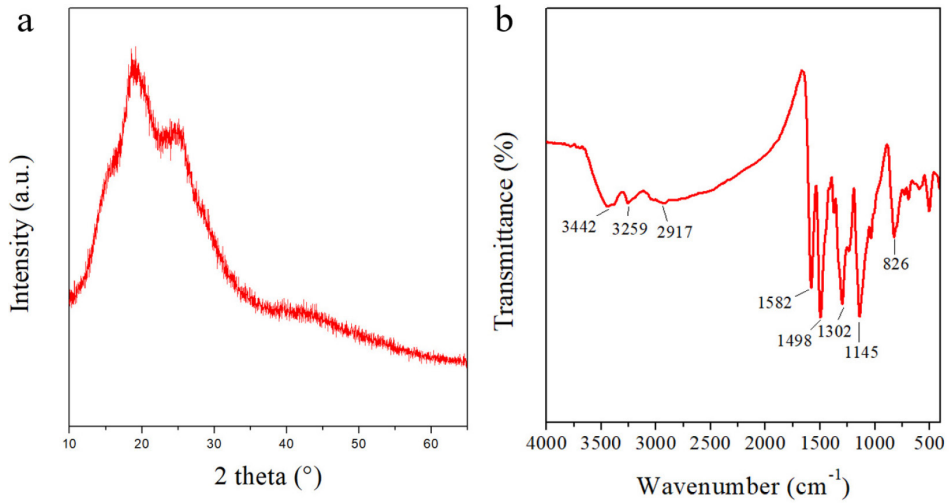

Figure 2. *(a) XRD pattern of polyaniline nanofibers; (b) FTIR spectra of polyaniline nanofibers*

Figure 3 displays four distinct quantitative correlations between the values of frequency shifts and BTEX concentrations (including 50, 100, 200, 400, and 800 ppb). The fitting equations for frequency shifts and concentrations of benzene, toluene, ethylbenzene, and xylene are: $y = -0.1961x - 3.929$ (determination coefficient (R^2) = 0.9995), $y = -0.2004x - 9.479$ (R^2 = 0.9998), $y = -0.1978x - 19.07$ (R^2 = 0.9952), and $y = -0.2048x - 20.33$ (R^2 = 0.9958), respectively. The preceding data suggests a linear proportionality in the frequency shifts across four equations. Referring to previous references,[42,43] the slope of regression equation is considered as sensitivity (ΔHz ppm^{-1}). Therefore, the sensitivity of the sensor to benzene, toluene, ethylbenzene, and xylene is –196.1, –200.4, –197.8, and –204.8 Hz ppm^{-1}, respectively. According to some review literature[22,44] on QCM gas sensors, it is known that a sensitivity greater than 10 Hz ppm^{-1} is already quite ideal. Therefore, the sensitivity of our sensor is appropriate.

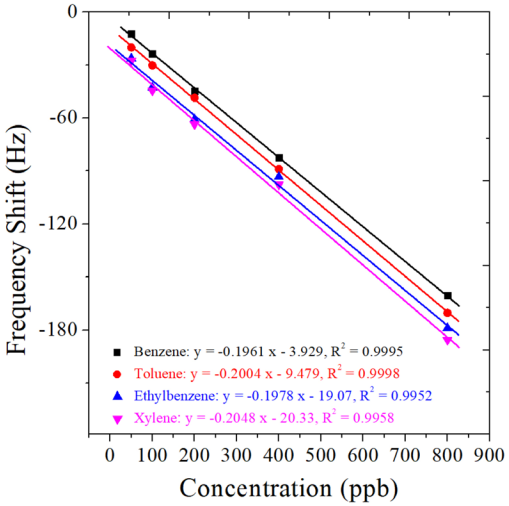

Figure 3. *Fitting curves of polyaniline nanofibers based QCM sensor with different concentrations of benzene, toluene, ethylbenzene, and xylene*

For gas sensors, attaining a level of selectivity is essential.[45] Testing of the polyaniline nanofibers based QCM sensor involved subjecting it to various typical gases including benzene, toluene, ethylbenzene, and xylene. Referring to Figure 4, the frequency shifts in the polyaniline nanofibers based QCM sensor were noticeable upon exposure to substances like benzene, toluene, ethylbenzene, xylene, acetone, CO_2, ethanol, and formaldehyde (HCHO) in a 50 ppb. It should be noted that the frequency shift values of this sensor for benzene (–12.3 Hz), toluene (–20.1 Hz), ethylbenzene (–26.3 Hz), and xylene (–27.7 Hz) at a concentration of 50 ppb are higher compared to the four interfering gases of acetone (–4.1 Hz), CO_2 (–3.6 Hz), ethanol (–2.8 Hz), and HCHO (–2.4 Hz). Consequently, although various other disruptive gases can induce a shift in frequency, these shifts are minor when contrasted with those caused by benzene, toluene, ethylbenzene, and xylene. It has been suggested that the adsorption mechanisms of aromatic compounds with polyaniline should be attributed to conjugated π-π electrons interactions.[46-48] Therefore, the polyaniline nanofibers based QCM sensor's enhanced adsorptive response to BTEX, four kinds of aromatic compounds, is likely due to the π-π electrons interactions occurring between the benzene ring structure of polyaniline and the benzene ring structure of aromatic BTEX.[49,50]

In Figure 5, the ongoing frequency shift of the polyaniline nanofibers based QCM sensor across four distinct gases is depicted, namely 50 ppb benzene, 50 ppb toluene, 50 ppb ethylbenzene, and 50 ppb xylene. Every frequency shift in this sensor demonstrates

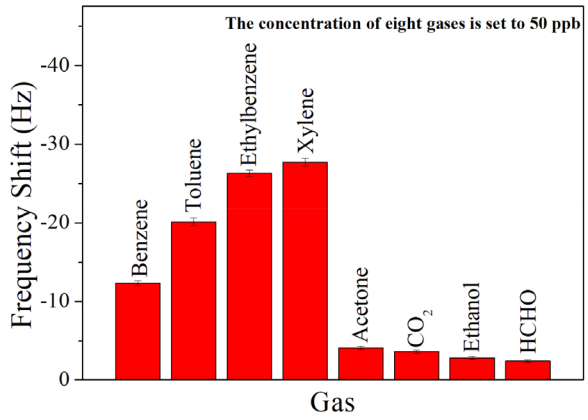

Figure 4. *Selectivity tests of polyaniline nanofibers based QCM sensor to 50 ppb of various detected gases at 298 K*

remarkable sensitivity and recuperation, signifying its consistent ability to detect various BTEX vapor types swiftly. Response time refers to the duration a sensor requires to reach 90% of the overall change in response frequency, while recovery time is the period it takes for a sensor to attain 90% of the total change in recovery frequency.[51] Polyaniline nanofibers based QCM sensors respond to 50 ppb benzene, 50 ppb toluene, 50 ppb ethylbenzene, and 50 ppb xylene in a timeframe of 22-38 s, with a recovery duration of 24-38 s, showcasing their rapid response and recovery potential.

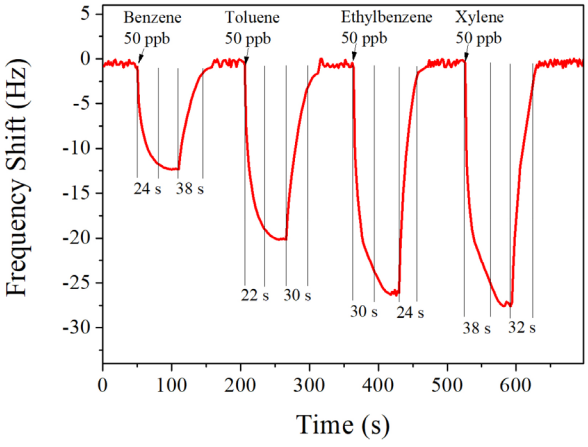

Figure 5. *The polyaniline nanofibers based QCM sensor exhibits continuous response curves, as well as the corresponding response time and recovery time, for 50 ppb benzene, 50 ppb toluene, 50 ppb ethylbenzene, and 50 ppb xylene*

The importance of moisture-resistance in gas sensors lies in its ability to reduce the impact of ubiquitous environmental humidity in practical applications on sensor performance, ensuring accurate and reliable detection results.[52] According to the water droplet contact angle test results shown in Figure 1b, the surface of polyaniline nanofibers based QCM sensor exhibits hydrophobicity. Therefore, we tested the frequency shift of the sensor under different humidity conditions (50-90% relative humidity). As shown in Figure 6, polyaniline nanofibers based QCM sensor exhibits stable frequency shift within the relative humidity range of 50-90% to vapor concentrations of 50 ppb of benzene, toluene, ethylbenzene, and xylene. This indicates that the sensor is capable of reliably detecting BTEX vapors at the ppb level in complex humidity environments.

For gas sensors, sustained stability serves as a crucial measure of performance.[53] In Figure 7, the enduring stability of polyaniline nanofibers based QCM sensor, against 50 ppb of benzene, toluene, ethylbenzene, and xylene at 298 K is depicted over a span of

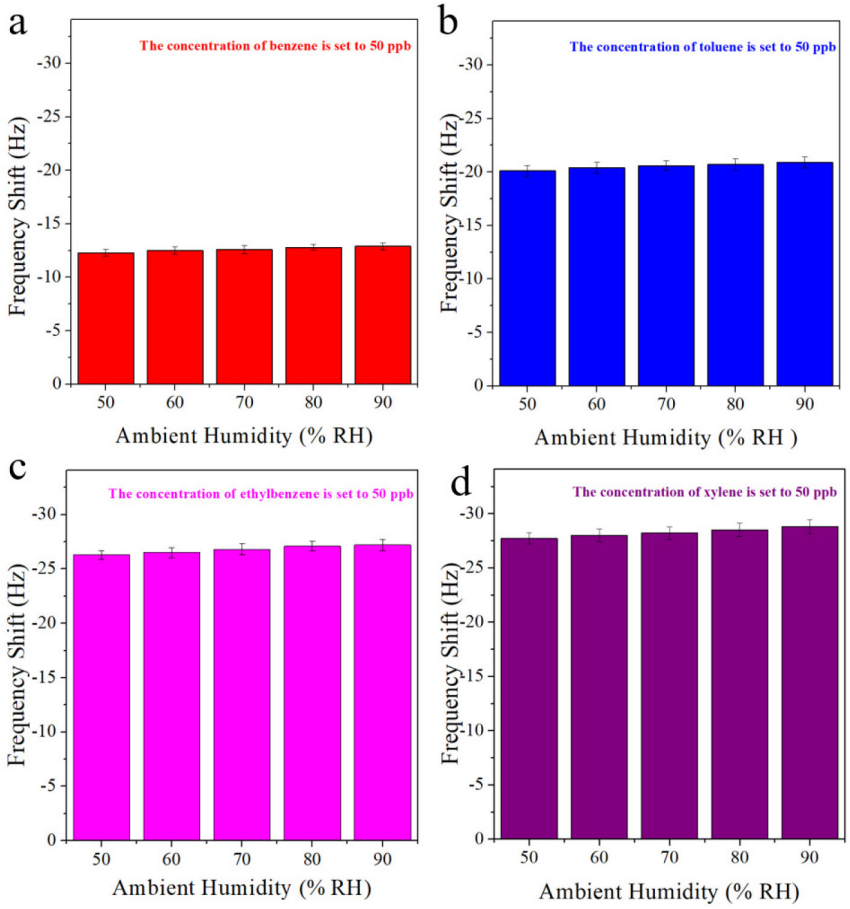

Figure 6. *The frequency shift values of polyaniline nanofibers based QCM sensor to different gases within the relative humidity range of 50-90%, including (a) 50 ppb benzene, (b) 50 ppb toluene, (c) 50 ppb ethylbenzene, and (d) 50 ppb xylene*

five weeks. Minimal variation in frequency shift was observed in the polyaniline nanofibers based QCM sensor at an identical concentration, signifying its remarkable stability over time.

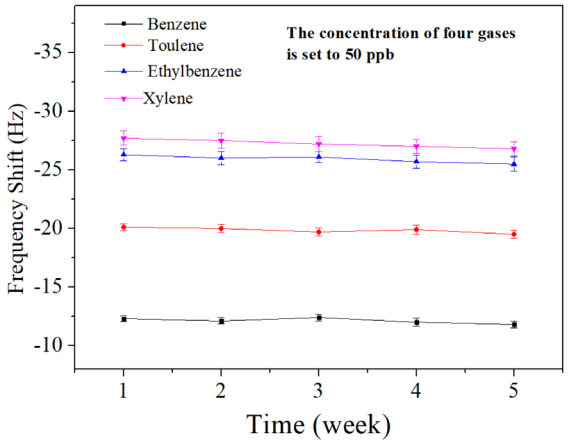

Figure 7. *The frequency shift values of the polyaniline nanofibers based QCM sensor to four different gases, including 50 ppb benzene, 50 ppb toluene, 50 ppb ethylbenzene, and 50 ppb xylene, over a period of five weeks*

CONCLUSIONS

In summary, we have utilized the QCM platform, with polyaniline nanofibers as the sensing material, to successfully detect BTEX vapors at ppb concentrations. The hydrophobic nature of the synthesized polyaniline allows for stable detection of BTEX vapors in different humidity environments. Additionally, the sensor exhibits excellent selectivity, fast response and recovery speed, as well as long-term stability. We believe that this work provides valuable insights and possibilities for the development of BTEX sensors with superior performance for practical applications.

SUPPLEMENTARY MATERIAL

The chemical raw materials and synthesis method of polyaniline nanofibers; characterization; fabrication and test methods of the QCM sensor; schematic of the gas testing system are available at http://quimicanova.sbq.org.br/, as a PDF file, with free access.

ACKNOWLEDGMENTS

This research was supported by National Natural Science Foundation of China under grant No. 62001420, Zhejiang Provincial Natural Science Foundation of China under grant No. LQ21F010017, University-Industry Collaborative Education Program under grant No. 220400576262052, and Science Foundation of Zhejiang Gongshang University Hangzhou College of Commerce, Zhejiang Gongshang University, China (ZJHZCC) under grant No. 2222111.

REFERENCES

1. Isinkaralar, K.; Turkyilmaz, A.; Lakestani, S.; *Environ. Technol. Innovation* **2023**, *31*, 103209. [Crossref]
2. Phillips, B.; Abani; Lin, H.; Wei, P.; Li, C.; Zhao, M.; Handy, J.; Banerjee, S.; Sue, H.-J.; Pentzer, E.; Al-Hashimi, M.; Zhou, H.-C.; Fang,

L.; *Mater. Today Chem.* **2022**, *24*, 100915. [Crossref]
3. Gong, X.; Hou, C.; Zhang, Q.; Li, Y.; Wang, H.; Serpe, M. J.; *ACS Appl. Opt. Mater.* **2023**, *1*, 860. [Crossref]
4. Asejeje, G. I.; Ipeaiyeda, A. R.; Onianwa, P. C.; *Environ. Sci. Pollut. Res.* **2021**, *28*, 15361. [Crossref]
5. Ojimelukwe, A. E.; Nafagha-Lawal, M. O.; Lelei, K. E.; Uche, A. O.; Kika, E. P.; Igbiri, S.; Babatunde, B. B.; Sikoki, F. D.; *Toxicol. Environ. Health Sci.* **2021**, *13*, 65. [Crossref]
6. Mokammel, A.; Rostami, R.; Niazi, S.; Asgari, A.; Fazlzadeh, M.; *Environ. Pollut.* **2022**, *298*, 118845. [Crossref]
7. Lu, F.; Li, S.; Shen, B.; Zhang, J.; Liu, L.; Shen, X.; Zhao, R.; *J. Hazard. Mater.* **2020**, *384*, 121428. [Crossref]
8. Liao, Q.; Zhang, Y.; Ma, R.; Zhang, Z.; Ji, P.; Xiao, M.; Du, R.; Liu, X.; Cui, Y.; Xing, X.; Liu, L.; Dang, S.; Deng, Q.; Xiao, Y.; *Environ. Pollut.* **2022**, *310*, 119894. [Crossref]
9. Szabó, I.; Varga, C.; *Int. J. Biometeorol.* **2020**, *64*, 989. [Crossref]
10. Al-Harbi, M.; Alhajri, I.; AlAwadhi, A.; Whalen, J. K.; *Atmos. Environ.* **2020**, *241*, 117847. [Crossref]
11. Sun, X.; Sun, Y.; Lyu, S.; Qiu, Z.; Sui, Q.; *Water Environ. Res.* **2020**, *92*, 622. [Crossref]
12. Tamrakar, A.; Pervez, S.; Verma, M.; Majumdar, D.; Pervez, Y. F.; Candeias, C.; Dugga, P.; Mishra, A.; Verma, S. R.; Deb, M. K.; Shrivas, K.; Satnami, M. L.; Karbhal, I.; *Water, Air, Soil Pollut.* **2022**, *233*, 411. [Crossref]
13. Dantas, G.; Gorne, I.; da Silva, C. M.; Arbilla, G.; *Bull. Environ. Contam. Toxicol.* **2022**, *108*, 204. [Crossref]
14. Zegebreal, L. T.; Tegegne, N. A.; Hone, F. G.; *Sens. Actuators, A* **2023**, *359*, 114472. [Crossref]
15. Li, Z.; Zeng, W.; Li, Q.; *Sens. Actuators, A* **2022**, *346*, 113845. [Crossref]
16. Dai, J.; Ogbeide, O.; Macadam, N.; Sun, Q.; Yu, W.; Li, Y.; Su, B.-L.; Hasan, T.; Huang, X.; Huang, W.; *Chem. Soc. Rev.* **2020**, *49*, 1756. [Crossref]
17. Majhi, S. M.; Mirzaei, A.; Kim, H. W.; Kim, S. S.; Kim, T. W.; *Nano Energy* **2021**, *79*, 105369. [Crossref]
18. Romih, T.; Menart, E.; Jovanovski, V.; Jerič, A.; Andrenšek, S.; Hočevar, S. B.; *ACS Sens.* **2020**, *5*, 2570. [Crossref]
19. Yang, B.; Myung, N. V.; Tran, T.-T.; *Adv. Electron. Mater.* **2021**, *7*, 2100271. [Crossref]
20. Rianjanu, A.; Fauzi, F.; Triyana, K.; Wasisto, H. S.; *ACS Appl. Nano Mater.* **2021**, *4*, 9957. [Crossref]
21. Son, J.; Ji, S.; Kim, S.; Kim, S.; Kim, S. K.; Song, W.; Lee, S. S.; Lim, J.; An, K.-S.; Myung, S.; *ACS Appl. Mater. Interfaces* **2021**, *13*, 4703. [Crossref]
22. Fauzi, F.; Rianjanu, A.; Santoso, I.; Triyana, K.; *Sens. Actuators, A* **2021**, *330*, 112837. [Crossref]
23. Shim, D.-Y.; Chang, S.-M.; Kim, J. M.; *Sens. Actuators, B* **2021**, *329*, 129143. [Crossref]
24. Wang, L.; *Sens. Actuators, A* **2020**, *307*, 111984. [Crossref]
25. Rianjanu, A.; Hasanah, S. A.; Nugroho, D. B.; Kusumaatmaja, A.; Roto, R.; Triyana, K.; *Chemosensors* **2019**, *7*, 20. [Crossref]
26. Iyer, A.; Mitevska, V.; Samuelson, J.; Campbell, S.; Bhethanabotla, V. R.; *Sensors* **2021**, *21*, 5667. [Crossref]
27. Temel, F.; Ozaytekin, I.; *Sens. Actuators, A* **2021**, *326*, 112688. [Crossref]
28. El Sabahy, J.; Berthier, J.; Ricoul, F.; Jousseaume, V.; *Sens. Actuators, B* **2018**, *258*, 628. [Crossref]
29. Ju, J.-F.; Syu, M.-J.; Teng, H.-S.; Chou, S.-K.; Chang, Y.-S.; *Sens. Actuators, B* **2008**, *132*, 319. [Crossref]
30. Bearzotti, A.; Macagnano, A.; Papa, P.; Venditti, I.; Zampetti, E.; *Sens. Actuators, B* **2017**, *240*, 1160. [Crossref]
31. Kumar, A.; Varenne, C.; Ndiaye, A. L.; Pauly, A.; Bouvet, M.; Brunet, J.; *Sens. Actuators, B* **2022**, *368*, 132253. [Crossref]
32. Abu-Thabit, N. Y.; *J. Chem. Educ.* **2016**, *93*, 1606. [Crossref]
33. Bhadra, S.; Singha, N. K.; Khastgir, D.; *J. Appl. Polym. Sci.* **2007**, *104*, 1900. [Crossref]
34. Li, D.; Huang, J.; Kaner, R. B.; *Acc. Chem. Res.* **2009**, *42*, 135. [Crossref]
35. Eskandari, E.; Kosari, M.; Farahani, M. H. D. A.; Khiavi, N. D.; Saeedikhani, M.; Katal, R.; Zarinejad, M.; *Sep. Purif. Technol.* **2020**, *231*, 115901. [Crossref]
36. Heme, H. N.; Alif, Md S. N.; Rahat, S. M. S. M.; Shuchi, S. B.; *Journal of Energy Storage* **2021**, *42*, 103018. [Crossref]
37. Shoaie, N.; Daneshpour, M.; Azimzadeh, M.; Mahshid, S.; Khoshfetrat, S. M.; Jahanpeyma, F.; Gholaminejad, A.; Omidfar, K.; Foruzandeh, M.; *Microchim. Acta* **2019**, *186*, 465. [Crossref]
38. Sambaza, S. S.; Maity, A.; Pillay, K.; *ACS Omega* **2020**, *5*, 29642. [Crossref]
39. Wang, J.; Wu, Y.; Cao, Y.; Li, G.; Liao, Y.; *Colloid Polym. Sci.* **2020**, *298*, 1107. [Crossref]
40. Ye, J. R.; Zhai, S.; Gu, Z. J.; Wang, N.; Wang, H.; Shen, Q.; *Mater. Lett.* **2014**, *132*, 377. [Crossref]
41. Yuan, J.; Hu, X.; Zhao, X.; Yin, J.; *Polymers* **2023**, *15*, 4568. [Crossref]
42. Haghighi, E.; Zeinali, S.; *RSC Adv.* **2019**, *9*, 24460. [Crossref]
43. Torad, N. L.; El-Hosainy, H.; Esmat, M.; El-Kelany, K. E.; Tahawy, R.; Na, J.; Ide, Y.; Fukata, N.; Chaikittisilp, W.; Hill, J. P.; Zhang, X.; El-Kemary, M.; Yamauchi, Y.; *ACS Appl. Mater. Interfaces* **2021**, *13*, 48595. [Crossref]
44. Torad, N. L.; Zhang, S.; Amer, W. A.; Ayad, M. M.; Kim, M.; Kim, J.; Ding, B.; Zhang, X.; Kimura, T.; Yamauchi, Y.; *Adv. Mater. Interfaces* **2019**, *6*, 1900849. [Crossref]
45. Wang, L.; Wu, Y.; Pan, Z.; Yu, C.; *Sens. Actuators, A* **2022**, *333*, 113296. [Crossref]
46. Sun, C.; Xiong, B.; Pan, Y.; Cui, H.; *J. Colloid Interface Sci.* **2017**, *487*, 175. [Crossref]
47. Shen, J.; Shahid, S.; Amura, I.; Sarihan, A.; Tian, M.; Emanuelsson, E. A. C.; *Synth. Met.* **2018**, *245*, 151. [Crossref]
48. Djellali, S.; Touati, A.; Semmeq, A.; Kebaili, M.; Badawi, M.; Bonilla-Petriciolet, A.; *Int. J. Chem. Eng.* **2022**, *2022*, 3181963. [Crossref]
49. Schneebeli, S. T.; Kamenetska, M.; Cheng, Z.; Skouta, R.; Friesner, R. A.; Venkataraman, L.; Breslow, R.; *J. Am. Chem. Soc.* **2011**, *133*, 2136. [Crossref]
50. Janiak, C.; *J. Chem. Soc., Dalton Trans.* **2000**, 3885. [Crossref]
51. Wang, L.; Xu, J.; Wang, X.; Cheng, Z.; Xu, J.; *Sens. Actuators, B* **2019**, *288*, 289. [Crossref]
52. Wang, L.; Yu, Y.; Xiang, Q.; Xu, J.; Cheng, Z.; Xu, J.; *Sens. Actuators, B* **2018**, *255*, 2704. [Crossref]
53. Karouei, S. F. H.; Moghaddam, H. M.; Niavol, S. S.; *J. Mater. Sci.* **2021**, *56*, 4239. [Crossref]